

# No-reference blur evaluation method for images based on edge analysis and segmentation in spatial domain using Canny Edge Detector

Hajera Siddiq<sup>1</sup>, Nusrat Ferdous<sup>2</sup>, Z. M. Parvez Sazzad<sup>3</sup>

<sup>1</sup>Department of Applied Physics, Electronics and Communication Engineering, University of Dhaka, Bangladesh.

E-mail: [hajerasiddiq@yahoo.com.au](mailto:hajerasiddiq@yahoo.com.au)

<sup>2</sup>Department of Electronics and Communication Engineering, Institute of Science and Technology, Bangladesh.

E-mail: [nferdous07@yahoo.com](mailto:nferdous07@yahoo.com)

<sup>3</sup>Department of Applied Physics, Electronics and Communication Engineering, University of Dhaka, Bangladesh.

E-mail: [sazzad@univdhaka.edu](mailto:sazzad@univdhaka.edu)

Author to whom correspondence should be addressed: E-mail: [nferdous07@yahoo.com](mailto:nferdous07@yahoo.com)

**Abstract--** In this research, a no-reference blur evaluation method has been developed for images based on edge analysis and segmentation in spatial domain. Blur mainly smoothes the image signal which causes the reduction of edge points. This edge information of an image can be estimated using canny edge detector. The perceptual blur of any image are strongly dependent on local features, such as plane and non-plane areas. Therefore, this local feature based edge detection is evaluated in this method. Subjective experiment results are used to verify this method. The outcomes indicate that the proposed method can efficiently predict blur of images.

**Index Terms-** No-reference, canny edge detector, DMOS, Segmentation, Blur-detection

## I. Introduction

Blur can be considered as the most frequent factor affecting image quality. Indeed blur is a common problem in most applications, such as in visual art, remote sensing, medical and astronomical imaging, as well as in machine vision. In order to improve the perceptual image quality, several objective quality metrics such as full reference (FR), reduced reference (RR) and no reference (NR) are used. Among these quality metrics, NR method is the most attractive since it does not need any prior knowledge about the reference image in order to assess the degraded one. This degradation or artifacts in a distorted image occurs due to blocking, ringing, noise, and blur.

Human vision and cognition easily evaluate image quality without the need for a reference image. Developing an objective image quality measure would require such a reference, which is rarely available. In developing a no-reference blur image quality measure, we seek to evaluate the image quality and to correlate it with the human vision system or with the effective introduced blur amount, without the need for an original image as a reference [1].

Because edges have usually high spatial frequency content, they are very sensitive to blur. Therefore, edge detection is a common step in most blur image quality measures. In literature, a number of blur metrics based on edge sharpness analysis have already been proposed. For example Marziliano *et al.* [2] developed a blur metric based on analyzing the edges width. The sharpness measurement index provided by Caviedes *et al.* [3] is based on local edge kurtosis. Chuang *et al.* [4] evaluate blur by fitting the image gradient magnitude to a normal distribution. L. Firestone *et al.* propose in [5], a frequency threshold metric based on computing the summation of all frequency component magnitudes above a fixed threshold. N. B. Nill *et al.* present in [6] an image quality metric (IQM) based upon calculating the normalized image power spectra weighted by a modulation transfer function. In [7] R. Fezli *et al.* developed a noise immune metric (NIS), based on image sharpness [8].



**Fig. 1: Reference image and its blur image.**

Here we are mainly concerned with NR blur assessment, which is an important problem in many applications. In addition, we integrate a significant human visual system characteristic based on local features such as different sensitivity of human eye on uniform (i.e., area with fewer edges) and non-uniform (i.e., area with more edges) areas [9]. Under the assumption that human visual perception is very sensitive to edge information of an image and any kinds of artifacts create pixel distortion, a discrimination algorithm is developed. The outcome of this proposal is evaluated by using Texas database [10].

## II. Proposed Model

An image appears blurred as shown in Fig. 1 when its high spatial frequency values in the spectrum are attenuated. The proposed no-reference blur measurement technique uses only luminance component of the coded image. Followed by block based segmentation for detecting edge block, the blurriness of the picture has been measured using canny edge detector. Finally, the blurriness values have been updated with weighting factors by using the Optimization algorithm. This proposed NR blur evaluation method based on edge analysis and segmentation is shown in Fig. 2.

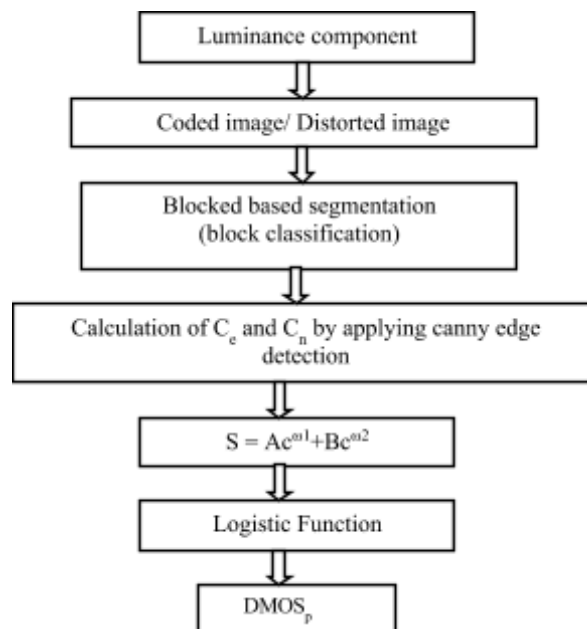


Fig. 2: NR objective Blur Evaluation Method

### A. Block Based Segmentation

In order to classify edge and non-edge blocks of an image, a simple block based segmentation algorithm is used [9, 11]. First, a simple pixel based segmentation method is established to classify each pixel within the image into either an edge, or non-edge pixel. Initially, standard deviation (STD) of each pixel is estimated within its 3x3 and 5x5 neighborhood pixels. For all corners, pixels that are taken into account are the only available pixels for the measures. Let  $STD_{3 \times 3}(m, n)$ , and  $STD_{5 \times 5}(m, n)$  be the standard deviated image of 3x3 and 5x5 neighborhood, respectively. Then we calculate absolute difference,  $D_a(m, n)$  by the following equation:

$$D_a(m, n) = |STD_{3 \times 3}(m, n) - STD_{5 \times 5}(m, n)| \quad (1)$$

Where,  $m = 1, 2, \dots, M$  denotes row and  $n = 1, 2, \dots, N$  denotes column. Subsequently, we calculate STD of  $D_a(m, n)$  by

$$D = \sqrt{\frac{\sum_{i=1}^{M \times N} (\bar{D}_a - D_{a_i})^2}{M \times N}} \quad D = \sqrt{\frac{\sum_{i=1}^{M \times N} (\bar{D}_a - D_{a_i})^2}{M \times N}} \quad \bar{D}_a = \sqrt{\frac{\sum_{i=1}^{M \times N} (D_{a_i} - \bar{D}_a)^2}{M \times N}} \quad (2)$$

We then use the following algorithm to classify edge and non-edge pixels of the image.

$$P(m, n) = \begin{cases} 1 & \text{if } D_a(m, n) \geq D \\ 0 & \text{otherwise} \end{cases}$$

Where, “1” and “0” denote edge and non-edge pixels respectively. Secondly, each block (8×8) of the image is classified into either edge or non-edge block by using the segmentation algorithm. The block based segmentation algorithm:

$$\text{Sum} = N_e + N_n \quad (3)$$

If  $\left(\frac{N_e}{N_e + N_n} > \text{th}_n\right)$  then the block is “edge”  
 else the block is “non – edge”.

Where,  $N_e$  and  $N_n$  are respectively the number of edge, and non-edge pixels per (8×8) block. Therefore, the “Sum” is the total number of pixels per block. Here, “ $\text{th}_n$ ” is the algorithmic threshold. The threshold estimation is described in details in Section IV. In this segmentation algorithm, threshold “ $\text{th}_n = 0.19$ ” is estimated empirically. It indicates that if more than 19% pixels within a block is edge, the block will be considered as “edge” block. Otherwise the block is defined as “non-edge” block.

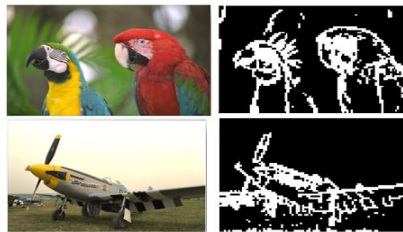


**Fig. 3:** Block based segmented images

We consider two color test images of size 640 × 512 and 24 bits *RGB*. The original and their corresponding block based segmented images are shown in Fig. 3.

### B. Canny Edge Detector

The Canny detector is the most powerful edge detector provided by function `edge` [12]. This method can be summarized as follows:

1. The image is smoothed using a Gaussian filter with a specified standard deviation,  $\sigma$ , to reduce noise.
2. The local gradient,  $g(x, y) = [\nabla_x^2 + \nabla_y^2]^{1/2}$  and edge direction,  $\theta(x, y) = \arctan\left(\frac{\nabla_y}{\nabla_x}\right)$  are computed at each point. Here,  $\nabla_x$  and  $\nabla_y$  are the first derivative of the pixel in x and y axis.
3. The edge points determined in (2) give rise to ridges in the gradient magnitude image. The algorithm then tracks along the top of these ridges and sets to zero all pixels that are not actually on the ridge top so as to give a thin line in the output, a process known as non-maximal suppression.
4. The ridge pixels are then threshold using two thresholds,  $T_1$  and  $T_2$ , with  $T_1 < T_2$ . Ridge pixels with values greater than  $T_2$  are said to be “strong” edge pixels. Ridge pixels with values between  $T_1$  and  $T_2$  are said to be “weak” edge pixels.

Finally, the algorithm performs edge linking by incorporating the weak pixels that are 8-connected to the strong pixels.

The MATLAB syntax for the Canny edge detector is

$$[c, t] = \text{edge}(f, \text{'canny'}, T, \text{sigma})$$

Where,  $T$  is a vector,  $T = [T_1, T_2]$ , containing the two thresholds explained in step 3 of the preceding procedure, and  $\text{sigma}$  is the standard deviation of the smoothing filter. If  $t$  is included in the output argument, it is two-element vector containing the two threshold values used by the algorithm. The default value for  $\text{sigma}$  is 1. Detail analysis of canny edge detector is explained in [12].

Our implementation uses the iterative approach. First all weak edges are scanned for neighbor edges and joined into groups. At the same time it is marked which groups are adjacent. Then all of these markings are examined to determine which groups of weak edges are connected to strong edges (directly or indirectly). All weak edges that are connected to strong edges are marked as strong edges themselves. The rest of the weak edges are suppressed. Fig. 4 shows the complete edge detection process with different threshold values where  $\text{sigma}$  is always 1.5.

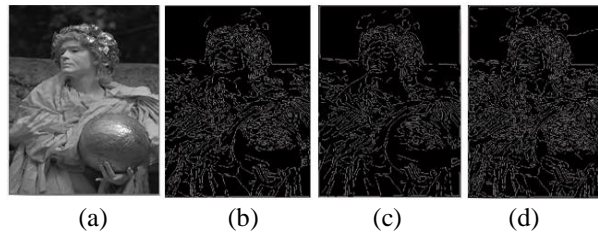


Fig. 4: Edged images by applying Canny edge detector. (a) original; (b)  $th_n[.04,0.1]$ ; (c)  $th_n[.06,.12]$  (d)  $th_n[0.01,.07]$ .

Now the total blur value or edge points of a block ( $8 \times 8$ ),  $B_{ij}$ , is calculated as follows:

$$B_{ij} = \sum_{p=1}^8 \sum_{q=1}^8 B(p, q)$$

Consequently, the average blurriness value of edge, and non-edge areas of the image are calculated by:

$$B_e = \frac{1}{N_e} \sum_{p=1}^{N_e} B_{p,p}$$

$$B_{ne} = \frac{1}{N_{ne}} \sum_{p=1}^{N_{ne}} B_{p,p}$$

Where,  $N_e$  and  $N_{ne}$  are respectively the number of edge, and non-edge blocks of the image. Again  $B_{e,p}$  and  $B_{ne,p}$  are the blur value of the corresponding blocks.

### III. Feature Combination

Our technique is based on the smoothing effect of blur on edges, and consequently attempts to measure the spread of the edges. We consider the following features combined equation:

$$F = W_1 B_e + W_2 B_{ne}^2$$

Where  $W_1$  and  $W_2$  are the method parameters. The method parameters and weighting factors  $W_1$  and  $W_2$  are must be estimated by an optimization algorithm with the subjective test data.

We consider a logistic function as the nonlinearity property between the human perception and the physical features. Finally, the obtained DMOS prediction,  $DMOS_p$ , is derived by the following equation.

$$DMOS_p = \frac{99}{1 + e^{-1.0217(F-50)}} + 1$$

(11)

Here, Particle Swarm Optimization (PSO) algorithm is used for the optimization [13].

### IV. Results and Discussions

It is clear from the segmentation algorithm ( section II) that the threshold value (“ $th_n$ ”) must be between 0-1. We select four different “ $th_n$ ” (0.16, 0.19, 0.25, 0.35) for all images which indicate the suitable threshold band of the proposed segmentation algorithm. As the target of this segmentation is used in the quality assessment, the best suitable threshold (“ $th_n$ ”) is estimated between the five values based on Spearman rank-order correlation coefficient (SROCC) between DMOS and DMOS predictions (DMOSP). In order to evaluate and verify the best suitable algorithmic threshold, we have considered our database and divided the database into two parts for training and testing. The training database consists of eleven randomly selected reference image (from the total twenty two) and all of their different combinations of coded images. The testing database consists of the other eleven reference images and their coded versions. For the verification, we can compare the performances of the algorithm using the different threshold values.

TABLE 1: Threshold performances based on Average absolute prediction error (AAE), Spearman rank-order correlation coefficient (SRO) and Pearson linear correlation coefficient (CC)

Th <sub>n</sub>	Training			Testing		
	AAE	SRO	CC	AAE	SRO	CC
0.16	7.46	0.93	0.79	16.48	0.73	0.70
0.19	7.05	0.94	0.84	14.07	0.79	0.80
0.25	7.2	0.93	0.8	14.1	0.79	0.80

5	6		1	8		
0.3	7.3	0.93	0.8	15.1	0.76	0.80
5	1		1	2		

Again, we have estimated all weighting factors ( $\omega_1$  and  $\omega_2$ ) and method parameters ( $\alpha$  and  $\beta$ ) for each threshold value separately by the optimization algorithm with the subjective test data. The calculated values for all training and testing images are shown in Table 1. The optimum threshold is estimated by comparing the performances of the algorithm with the different threshold values based on minimum value of AAE and maximum value of SROCC. Therefore, in all cases (in Table 1), the performance of the segmentation algorithm is very good with the threshold value of “ $th_n$ ” = 0.19. The obtained method parameters and weighting factors by the PSO optimization algorithm for the threshold value of our training database (DMOS scale,0-100) are shown in Table 2.

**TABLE 2: Method parameters and weighting factors for quality scale, 0-100**

$\alpha = -13.3801$	$\beta_1 = .0047$
$\beta = 59.3801$	$\beta_2 = 0.2012$

In Fig. 3, the white and dark blocks are respectively indicating edge and non-edge blocks in the segmented images. This indicates sufficient segmentation performance. Though, this segmentation is used to improve quality prediction performance, it is not an exactly accurate segmentation. Because, if any block contains same type of pixels (either edge or non-edge), the block then ideally considers as either edge or non-edge.

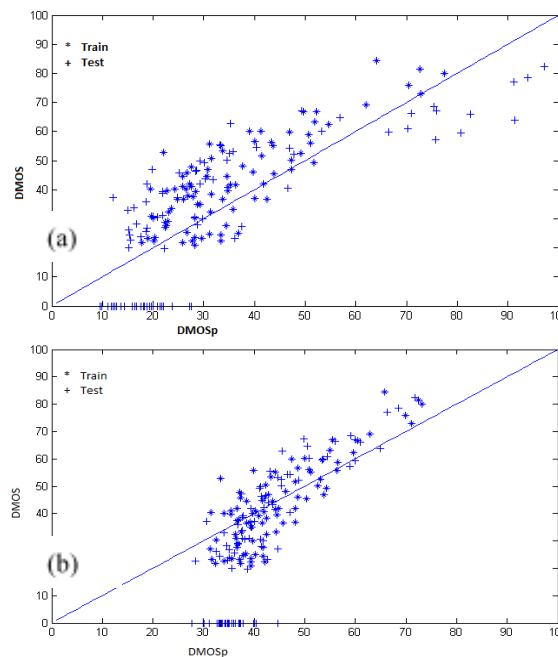


**Fig. 5: Scatter plot of difference mean opinion score (DMOS) versus DMOS prediction of the blurred image dataset in LIVE database where (a) contain 0.19 threshold and (b) contain 0.25 threshold. Each data point represents one test image.**

Otherwise, it is very difficult to identify accurately the type of blocks. We can say from Fig. 3 that low level pixel variations areas are non-edge areas (dark blocks) and the others areas are edge areas (white blocks) [11].

Now the DMOS versus DMOSp of our proposed model for training and testing images are respectively shown in Fig. 5(a) and 5(b). The symbols ‘+’ and ‘\*’ respectively indicate MOSp points for the databases of training and testing.

We have done our experiment with Gaussian blurred images. At first we have calculated trained value and then taking the value of  $\alpha$ ,  $\beta$ ,  $\omega_1$  and  $\omega_2$  from our first calculation. Then we have determined test value. Graph shows that our experiment nearly accurate.

Now we have taken three images of butterfly which are compressed according to different compression level. We will observe that DMOS value from data base of these images how much differs from prediction value of DMOS, which we have obtained from our proposed model.

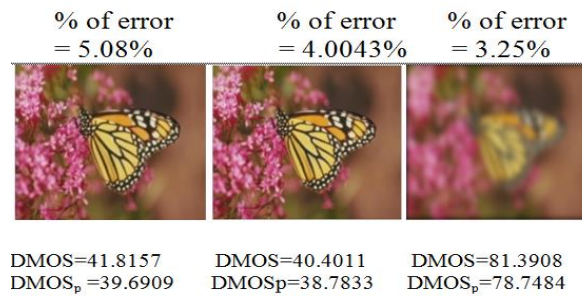


**Fig. 6: Original image of Butterfly and its different compression level by Gaussian Blur**

Three different compressed images of butterfly and also their DMOS, DMOS<sub>p</sub> values with percentage of error are shown in Fig. 6.

### V. Conclusions

We have proposed no reference blur measurement objective method of compressed image. Canny edge detector function is applied to detect edge of the image. We have measured blur of a Gaussian blurred image which is near real-time and has low computational complexity. Its performance is independent of the image content. Applications of this metric involve source coding optimization, network resource management and auto-focusing of a capturing device. Future research includes the measurement of other type of artifacts such as ringing.

### REFERENCES

- [1] Z. Wang, Hamid R. Sheikh and A. C. Bovic: No- reference perceptual quality assessment of JPEG compressed images. Proc. IEEE Int. Conf. Image Processing, Rochester, pp. 477- 480, NY (2002).
- [2] P. Marziliano, F. Dufaux, S. Winkler, T Ibrahim: A no reference perceptual blur. International conference on image processing Rochester, NY (2002)
- [3] J. Caviedes, S. Gurbuz : No reference sharpness metric based on local edges Kurtosis. IEEE international conference on image processing, Rochester NY (2002).
- [4] Y. Chung, Y. J. Bailey, S. Chen, S. Chang : A nonparametric blur measure based on edge analysis for image processing applications. IEEE conf Cybern intell syst 1:356-360 (2004).
- [5] L. Firestone, Cook, N. Talsamia and K. Preston: Comparison of autofocus methods of automated microscopy. Citometry, vol. 12, pp. 195-206 (1991).
- [6] N. B. Nill, B. H Bouzas: Objective image quality measure derived from digital image power spectra. Opt, Eng, vol. 31, no 4, pp. 813-825, Nov(1992).
- [7] R. Fezli, L. J. Karem : No reference objective wavelet based noise immune image sharpness metric. IEEE International Conference on Image Processing. Vol. 1, PP. 405-408, Sept (2005).
- [8] F. Kerouh, A. Serir, "A No Reference Quality Metric for Measuring Image Blur In Wavelet Domain ", International Journal of Digital Information and Wireless Communications (IJDIWC) 1(4): 767-776, The Society of Digital Information and Wireless Communications, 2011 (ISSN 2225- 658X)
- [9] Z. M. Parvez Sazzad, Y. Horita "Local region-based image quality assessment independent of JPEG and JPEG2000 coded color images" vol.23, pp.257-268, Jul.18,2008.
- [10] Laboratory for Image and Video Engineering, (LIVE data base), The university of Texas, Austin.
- [11] Z. M. Parvez Sazzad "NO-Reference Image Quality Assessments For JPEG and JPEG2000 Coded image", PhD thesis, March 2008.
- [12] Rafael C. Gonzalez , "Digital Image Processing Using MATLAB", ISBN 81-7758-898-2.
- [13] J. Kennedy and R. Eberhart, "Particle Swarm Optimization," Proc. IEEE ICNN, Pearth, Australia, pp. 1942-1948.